

2005 HST Calibration Workshop
 Space Telescope Science Institute, 2005
 A. Koekemoer, P. Goudfroiij, and L. Dressel, eds.

Modeling and Correcting the Time-Dependent ACS PSF

Jason Rhodes

Jet Propulsion Laboratory, 4800 Oak Grove Drive, Pasadena, CA 91109

Richard Massey, Justin Albert, James E. Taylor

California Institute of Technology, 1200 East California Blvd, Pasadena, CA 91125

Anton M. Koekemoer

Space Telescope Science Institute, 3700 San Martin Drive, Baltimore, MD, 21218

Alexie Leauthaud

*Laboratoire d'Astrophysique de Marseille, BP 8, Traverse du Siphon, 13376
 Marseille Cedex 12, France*

Abstract. The ability to accurately measure the shapes of faint objects in images taken with the *Advanced Camera for Surveys* (ACS) on the *Hubble Space Telescope* (HST) depends upon detailed knowledge of the Point Spread Function (PSF). We show that thermal fluctuations cause the PSF of the ACS Wide Field Camera (WFC) to vary over time. We describe a modified version of the *TinyTim* PSF modeling software to create artificial grids of stars across the ACS field of view at a range of telescope focus values. These models closely resemble the stars in real ACS images. Using ~ 10 bright stars in a real image, we have been able to measure HST's apparent focus at the time of the exposure. *TinyTim* can then be used to model the PSF at any position on the ACS field of view. This obviates the need for images of dense stellar fields at different focus values, or interpolation between the few observed stars. We show that residual differences between our *TinyTim* models and real data are likely due to the effects of Charge Transfer Efficiency (CTE) degradation. Furthermore, we discuss stochastic noise that is added to the shape of point sources when distortion is removed, and we present *MultiDrizzle* parameters that are optimal for weak lensing science. Specifically, we find that reducing the *MultiDrizzle* output pixel scale and choosing a Gaussian kernel significantly stabilizes the resulting PSF after image combination, while still eliminating cosmic rays/bad pixels, and correcting the large geometric distortion in the ACS. We discuss future plans, which include more detailed study of the effects of CTE degradation on object shapes and releasing our *TinyTim* models to the astronomical community.

1. Introduction and motivation

Accurate shape measurements of faint, small galaxies are crucial for certain applications, most notably the measurement of weak gravitational lensing. Quantifying the slight distortion of background galaxies by foreground matter relies on detecting small but coherent changes in the shapes of many galaxies (see Refregier 2003 for a recent review). To extract the lensing signal, it is crucial to remove instrumental effects from galaxies' measured shapes. On the *Hubble Space Telescope* (HST), these include:

- Convolution of an image with the telescope’s Point Spread Function (PSF).
- Geometric distortion of an image. This is particularly large in the *Advanced Camera for Surveys* (ACS) because of its location off HST’s optical axis.
- Trailing of faint objects in the CCD readout direction due to degraded Charge Transfer Efficiency (CTE).

In this proceeding, we describe a method to model and correct for the telescope’s temporally and spatially varying PSF. The geometric distortion has already been shown to be successfully removed during image processing by *MultiDrizzle* (Koekemoer et al. 2002). Removing the distortion does change the PSF, and we present recommendations to minimize stochastic changes introduced during the repixelization stage of image processing. The effect of continuing CTE degradation on galaxy shapes is only becoming apparent as the ACS spends longer in orbit, and is not yet completely understood. That is therefore beyond the scope of this proceeding. A separate method to remove CTE effects will be presented in Rhodes et al. (2006), and the application of all these corrections in a weak lensing analysis will be presented in Massey et al. (2006). Other branches of astronomy, including stellar photometry in crowded fields, the study of AGN, and proper motions also require detailed knowledge of the PSF and will benefit from the models we describe here.

In weak lensing, to deconvolve galaxy shapes from the PSF, we must accurately know the shape of the PSF at the position of the object and at the time of the observation. For example, see Rhodes, Refregier & Groth (2000) for a description of the method we use on the Cosmic Evolution Survey (COSMOS; Scoville et al. 2006) images we use to test the PSF models we describe in this paper. If the HST PSF were stable over time, it would be straightforward to build a catalog of stellar images across the entire field of view. However, thermal fluctuations in HST that change its effective focus (the distance between the primary and secondary mirrors) lead to temporal PSF variations. As an example, Figure 1 shows the PSF pattern in two sets of COSMOS images. The left hand panel shows stars from images taken when the telescope was near optimal focus, and the right hand panel shows stars observed when the telescope was several microns below optimal focus. Each tick mark in the figure represents the ellipticity of one star, measured using the standard weak lensing definition,

$$|e| = \frac{[(I_{xx} - I_{yy})^2 + (2I_{xy})^2]^{1/2}}{I_{xx} + I_{yy}}, \quad (1)$$

where star’s weighted second order moments

$$I_{ij} = \frac{\sum w I x_i x_j}{\sum w I} \quad (2)$$

involve summations over all pixels. I is the intensity of a pixel, w is some weighting function (in our case a Gaussian with a width of about the FWHM of the PSF), and x_i is the distance of a pixel from the centroid of the object. It is apparent from Figure 1 that changes in the PSF over time are sufficient for a temporally stable ACS PSF model to be inadequate in demanding applications, when using data collected over a period of more than a few days. Other effects, including CTE, introduce additional variation on longer time scales.

This proceeding is organized as follows. In §2. we introduce the *TinyTim* software package that we used for PSF modeling, and discuss modifications that we have made. In §3. we discuss *MultiDrizzle* and how to minimize the aliasing of point sources that occurs during distortion removal. In §4. we show how we have used our *TinyTim* models to quantify the temporal variation of the ACS PSF, and describe how the same models can be used to correct for it. In §5. we draw conclusions and outline a plan to release our *TinyTim* PSF models.

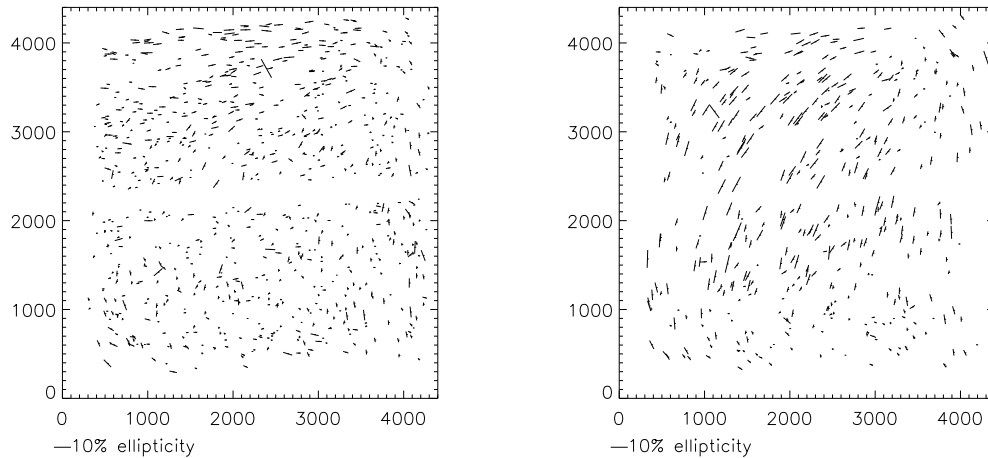


Figure 1.: The ellipticity of stars in the COSMOS survey observed with the ACS WFC while HST happened to be at nominal (left panel) and low (right panel) focus. The orientation and size of each tick mark represents the ellipticity of one star; both panels contain stars from several different fields. The difference in the PSF patterns is apparent, and demonstrates the need for a time dependent PSF model.

2. TinyTim PSF models

We have adapted version 6.3 of the *TinyTim* software package (Krist & Hook 2004) to create simulated images of stars. *TinyTim* creates FITS images containing one or more stars that include the effects of diffraction, geometric distortion, and charge diffusion within the CCDs. By default the images appear as they would in raw ACS data; they are highly distorted and have a pixel scale of 0.05 arcseconds per pixel. We have written an IDL wrapper to undo the distortion, resample the images, and combine adjacent PSFs to mimic the effects of dithering. The wrapper can also run *TinyTim* multiple times and create a grid of PSF models across the whole ACS field of view. We insert our artificial stars into blank images with the same dimensions and FITS structure as real ACS data, thereby manufacturing arbitrarily dense starfields.

This basic pipeline calculates a diffraction pattern (spot diagram), distorts it, and adds charge diffusion; all three effects usually depend upon the position of the star in the ACS field of view. We have made two versions of artificial starfields with important changes to this basic pipeline. The deviations from this default are:

- In order to examine the effects of the distortion removal process, we have created a version of our *TinyTim* starfields where each star has an identical diffraction pattern and charge diffusion, but a geometric distortion determined by the location of the PSF within the ACS field of view. Once the geometric distortion is removed (for example by running the field through *MultiDrizzle*), these stars should all appear identical.
- In order to correct data, we have created a second version of our *TinyTim* starfields that do not contain the effects of geometric distortion at all, instead modeling stars as they would appear after a perfect removal of geometric distortion. Conversion between distorted and non-distorted frames, which is necessary to simulate charge diffusion in the raw CCD, was performed using very highly oversampled images. This avoids stochastic aliasing of the PSF (see §3.), and minimizes noise in the PSF models.

We describe the application of these simulations in the following two sections.

3. Optimization of MultiDrizzle parameters for Weak Lensing Science

MultiDrizzle is used to combine dithered exposures, remove cosmic rays and bad pixels, and eliminate the large geometric distortion in ACS WFC images (Koekemoer et al. 2002). However, the transformation of pixels from the distorted input image to the undistorted output plane can introduce significant “aliasing” of pixels if the output pixel scale is comparable to the input scale. When transforming a single input image to the output plane, point sources can be enlarged, and their ellipticities changed by several percent, depending upon their sub-pixel position. This is one of the fundamental reasons why dithering is recommended for observations, since the source is at a different sub-pixel position in different exposures, hence the effects are mitigated to some extent when all the exposures are combined. However, the remaining effect in combined images is still quite sufficient to prevent the measurement of small, faint galaxies at the precision required for weak lensing analysis.

Of course, such pixellization effects are unavoidable during the initial exposure, when the detector discretely samples an image. However, it is clearly desirable to minimize related effects during data reduction. The effect on each individual object depends on how the input and output pixel grids line up. Indeed, this can be mitigated by using a finer grid of output pixels (*e.g.* Lombardi et al. 2005). The reduction in pixel scale (which will cause a corresponding increase in computer overheads) can be performed in conjunction with simultaneously “shrinking” the area of the input pixels that contains the signal, by making use of the *MultiDrizzle* `pixfrac` parameter and convolution kernel.

We have run a series of tests on the simulated PSF grids described in §2. to determine the optimal values of the *MultiDrizzle* parameters specifically for weak lensing science. To this end, we first produced a grid of stars that ought to look identical after the removal of geometric distortion. Figure 2 shows the “aliasing” produced when the distortion is removed from a single image. We have also created a series of four dithered input images (with the linear dither pattern used for the COSMOS survey); the scatter in the ellipticities of the output stars is then approximately half as big. This confirms the idea that the repixellization adds stochastic noise to the ellipticity when the four sub-pixel positions are uncorrelated. For weak lensing purposes, this noise is still substantial. With enough dithered input images, the scatter of ellipticities could be reduced further, but this is not feasible for most observations.

We then ran a series of tests using *MultiDrizzle* on the same input image but with a range of output pixel scales, convolution kernels, and values of `pixfrac`. We then measured the scatter in the ellipticity values in the output images. The smaller that scatter, the more accurately the PSF is represented. We found the results were not strongly dependent on the choice of `pixfrac` and settled on a value of 0.8 for that parameter. We show in Figure 3 that PSF stability is improved dramatically by reducing the output pixel scale from 0.05 arcseconds (the default) to 0.03 arcseconds. There is only a very slight gain in going to smaller output pixel sizes and the storage requirements rapidly become problematic. The gain in going to smaller pixel scales is more stable with a Gaussian kernel for than with the default square kernel. Therefore, for weak lensing work, we recommend an output pixel scale of 0.03 arcseconds, `pixfrac`=0.8, and a Gaussian kernel in order to best preserve the PSF during this stage of image reduction. We note that, despite its clear advantages for weak lensing studies, the Gaussian kernel does have some general drawbacks, such as the introduction of more correlated noise which may not be desirable for other types of science where minimization of correlated noise is important.

4. Quantification of the PSF and focus variability

We can measure HST’s effective focus at the time of an observation using ~ 10 fairly bright stars in the field. We first created dense grids of artificial stars across the ACS field

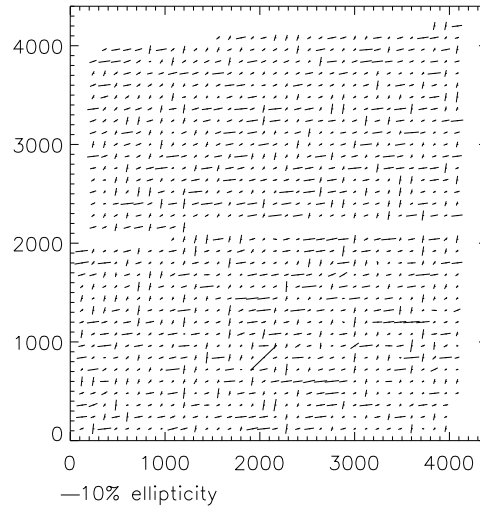


Figure 2: “Aliasing” of the PSF introduced when transforming a single distorted input image to the undistorted output frame. The tick marks represent the ellipticity of stars that have undergone identical diffraction in the telescope’s optics and should therefore look identical. The only difference between stars is their sub-pixel position when their geometric distortion is removed and the images are combined. The apparent difference between the tick marks shows that the PSF is changed. The problem can be ameliorated by altering several of the *MultiDrizzle* settings, in particular reducing the output pixel scale.

of view. By changing the separation of the primary and secondary mirrors in *TinyTim*’s raytracing model, these models were made at successive displacements of the focus from nominal, from $-10\mu\text{m}$ to $+5\mu\text{m}$ in $1\mu\text{m}$ increments. These are reasonable bounds on the maximum extent of physical variations in HST. The stars are created without geometric distortion, to avoid the noise that would have been introduced had it been necessary to carry out geometric transformations on the stellar fields. We then compare the ~ 10 bright stars in each COSMOS field to the *TinyTim* PSF grids at each focus value. Minimizing the difference in ellipticity between the models and the data finds the best fit value of telescope focus for that particular field. Tests on observations of dense stellar fields that contain many suitable stars show that this procedure is repeatable with an rms error $\sim 1\mu\text{m}$, when using ten different stars repeatedly selected at random.

Figure 4 shows our estimation of HST’s focus in microns away from nominal during several months in Cycles 12 and 13, using a uniform set of COSMOS images. HST was not manually refocussed during this time, but the apparent focus still oscillates. At times, the oscillations seem periodic, but there are also sharp jumps and more erratic behavior. The random component probably depends in a complex fashion upon the orientation of HST with respect to the sun and the Earth during preceding exposures, and we do not believe that it can be easily predicted in advance.

Note that the uncertainty on the focus value during any single pointing is quite large; more so than the tests on dense stellar fields would suggest. A major component of this error is undoubtedly the $\sim 3\mu\text{m}$ thermal fluctuations in focus that HST experiences during each orbit due to “breathing”. The COSMOS images are all taken with a total exposure time of one orbit, and the apparent focus therefore represents the integral of a gradually changing PSF. We have not been able to investigate focus changes on short time periods and, given this behavior, it is even more curious that long term patterns are so clearly present in Figure 4.

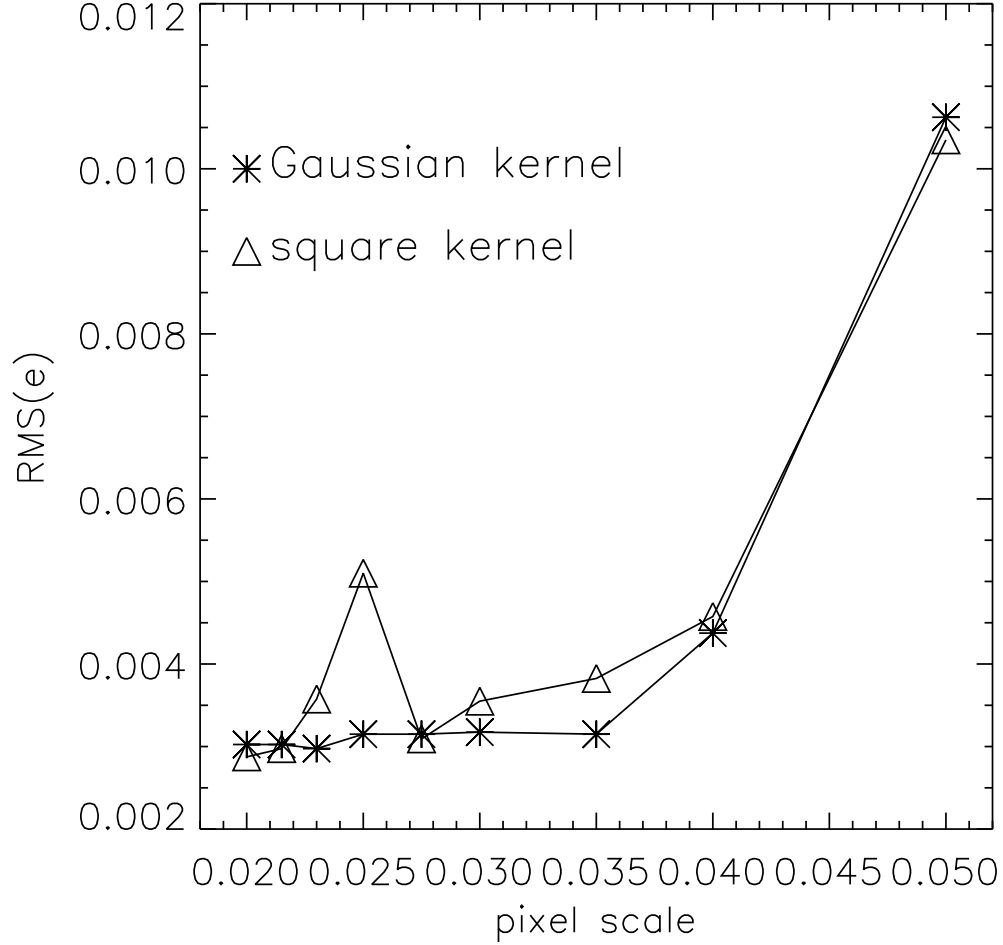


Figure 3.: RMS ellipticity introduced during the process of removing geometric distortion and combining dithered images, for a range of *MultiDrizzle* parameters. Lower values show more stable behavior of the PSF during this process. Based on this plot, we recommend a Gaussian kernel and an output pixel size of 0.03 arcseconds in order to minimize the effect of undersampling on the PSF and produce images that are optimal for weak lensing science. We note that the Gaussian kernel introduces significant additional correlated noise relative to the square kernel, which is not important for weak lensing science but may not be optimal for other types of science.

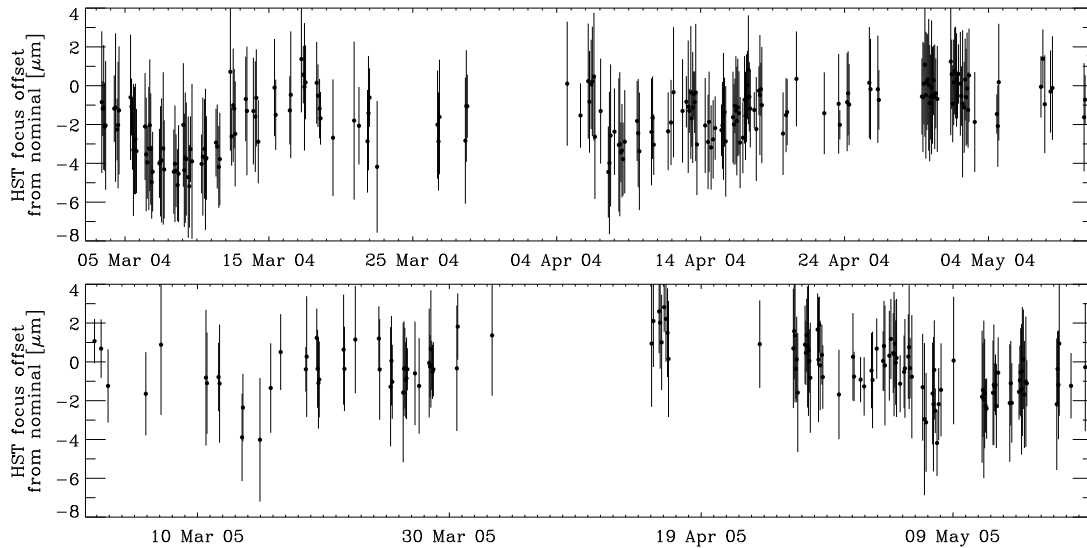


Figure 4.: Apparent offset of HST from nominal focus during COSMOS observations in cycles 12 and 13. We describe the procedure by which we estimate the telescope’s focus in §4.

Figure 5 shows the focus values determined for all of the COSMOS fields. The obvious clustering of focus values in that plot is due to the observing strategy used for COSMOS, in which data was typically taken in chunks of a few fields at a time. Adjacent fields are likely to have been taken at similar times, and therefore tend to have a similar focus values.

Figure 6 shows the *TinyTim* models at focus $-3\mu\text{m}$ and all the stars from the COSMOS fields with a best-fit focus value of $-3\mu\text{m}$. The COSMOS stars have been averaged in a spatial grid of approximately 600×600 0.03 arcsecond pixels. There is good agreement between the models and the stars over most of the field. The agreement is not as good in the boxed area near the center of the field. We believe this is due to a degradation of the CTE of the ACS CCDs. This degradation causes trailing of low flux objects in the readout direction (the y direction). The effect is most pronounced the further away the object is from the readout registers at the bottom and top of the field (Mutchler & Sirianni 2005; Riess & Mack 2004). This causes the objects to be elongated vertically. Thus, fainter COSMOS stars appear more elongated in the y direction at the center of the field than the *TinyTim* models, which do not include the effects of CTE. Note that this does not affect the estimation of focus positions, because the bright stars matched to our PSF models are less affected by CTE than the faint sources. We are currently exploring ways to correct for CTE in all objects, and will publish the results in Rhodes et al. (2006).

5. Conclusions and Future Work

We have shown that *TinyTim* can produce model PSFs that are very close to those observed in real data (for example the COSMOS 2-Square Degree Survey). This required some modifications to the *TinyTim* code, most importantly adding the ability to mimic the distortion correction and dithering normally implemented via *MultiDrizzle*, and to produce grids of PSFs across the entire ACS WFC field of view. We used *TinyTim* model stars to find the best values for *MultiDrizzle* and found that using a Gaussian kernel, $\text{pixfrac} = 0.8$, and an output pixel scale of 0.03 arcseconds greatly reduced the “aliasing” of point sources introduced during repixellization.

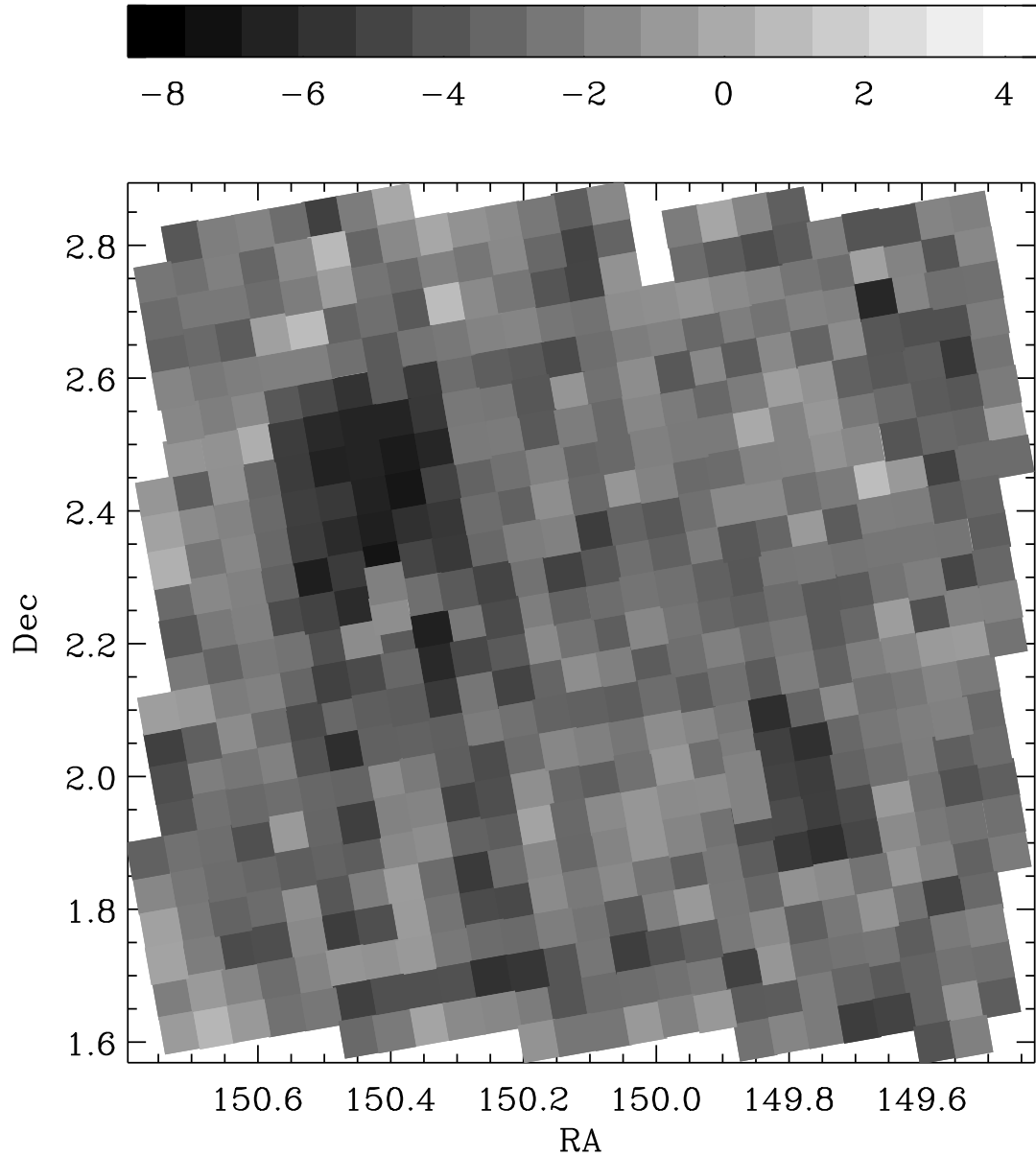


Figure 5.: Apparent offset of HST from nominal focus in all of the COSMOS fields. COSMOS was taken in chunks, a few fields at a time. Therefore, the focus values cluster because fields taken close to each other in time tend to have similar focus values. Despite having only about 10 stars per COSMOS field which are suitable for measuring PSF, it is apparent from the clustering of focus values in this plot that we can make a decent estimate of the focus value for individual COSMOS fields using the models and techniques outlined in this paper.

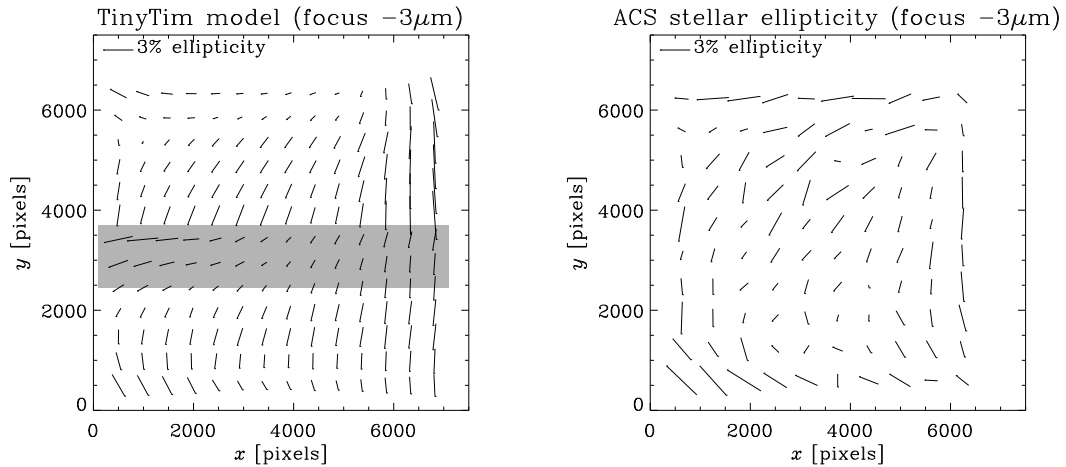


Figure 6.: The *TinyTim* PSF models (left panel) for a focus value of $-3\mu\text{m}$ and observed stars (right panel) in COSMOS fields with a similar apparent focus. There is good agreement between the data and the models over much of the ACS field. The shaded area near the center of the chip does not show good agreement and this is likely due to the effects of degradation of the Charge Transfer Efficiency (CTE) in the ACS WFC CCDs.

Discrepancies between our models and the COSMOS data can be attributed largely to a degradation in the ACS CTE since launch. We are currently studying this problem and will present a complete PSF solution including how to correct for CTE in Rhodes et al. (2006). We plan to correct science images for CTE on a pixel-by-pixel basis, like the Bristow code developed for STIS (Bristow et al./ 2002), moving charge back to where it belongs, rather than including the effects of CTE in our model PSF (like Rhodes et al. 2004). Thus, the model PSFs we present here are the ones we plan to use in our weak lensing analysis.

At the time of press, we have thoroughly tested PSF models in only the F814W filter. However, our IDL routines preserve *TinyTim*'s ability to create PSFs in other filters, and for sources of any colors. Our routines are therefore easily adaptable to other data sets.

The whole method is intentionally designed to be as adaptable as possible for many methods. The desire to know the PSF at any arbitrary position on the sky is far from unique to weak lensing. But even in lensing, advanced methods like Shapelets will, in the near future, be able to take advantage of more detailed information about the PSF shape than it is reasonable to expect from interpolation between a few stars (Massey & Refregier 2005; Refregier & Bacon 2004). This is even more exaggerated when considering higher order shape parameters, with an intrinsically lower signal to noise. The creation of noise-free, oversampled stars at any position on an image allows such analysis in any ACS data.

In the near future, we plan to release our PSF models to the community along with the wrapper we have written for *TinyTim* which will allow users to create PSF models in different filters and at user-defined positions in the ACS field of view. Interested readers are advised to contact the authors for these resources.

Acknowledgments. We would like to thank Catherine Heymans for sharing her knowledge of the ACS PSF. We are grateful to John Krist for guiding our poor lost souls through the underbelly of *TinyTim*. Great thanks go to Andy Fruchter and Marco Lombardi for useful discussions about *MultiDrizzle*. Adam Riess and Marco Sirianni provided expert knowledge about CTE effects. Richard Ellis and Alexandre Refregier have engaged us in many useful and interesting discussions about the COSMOS field. We are also pleased to acknowledge the continuing support of Nick Scoville, Patrick Shopbell and the whole COS-

MOS team in obtaining and analyzing the COSMOS images that were used to test our PSF models.

References

- Bristow et al. 2002, *Modelling Charge Transfer on the STIS CCD*, in *The 2002 HST Calibration Workshop : Hubble after the Installation of the ACS and the NICMOS Cooling System*, Eds Arribas, Koekemoer, & Whitmore, STScI
- Koekemoer, A. M., Fruchter, A., Hook, R. & Hack, W., 2002, ‘MultiDrizzle: An Integrated Pyraf Script for Registering, Cleaning and Combining Images,’ in *The 2002 HST Calibration Workshop : Hubble after the Installation of the ACS and the NICMOS Cooling System*, Eds Arribas, Koekemoer, & Whitmore, STScI, p. 337
- Krist, J. & Hook, R., 2004, ‘The TinyTim User’s Guide’, STScI, 339
- Lombardi, M. et al., 2005, *ApJ*, 623, 42
- Massey R. & Refregier, A. 2005, *MNRAS* 363, 197
- Massey R. et al. 2006, in preparation
- Mutchler, M. & Sirianni, M., 2005, *Instrument Science Report ACS 2005-003*, (Baltimore: STScI), available through <http://www.stsci.edu/hst/acs>
- Refregier, A., 2003, *ARA&A*, 41, 645
- Refregier, A. & Bacon, D., 2002, *MNRAS*, 338, 48
- Rhodes, J. et al. 2006, in preparation
- Rhodes et al. 2004, *ApJ*, 605, 29
- Rhodes, J., Refregier, A. & Groth, E., 2000, *ApJ*, 536, 79
- Riess, A. & Mack, J., 2004, *ISR ACS 2004-006*, STScI
- Scoville, N. et al. 2006, in preparation